Communications in Physics, Vol. 27, No. 2 (2017), pp. 151-164
DOI:10.15625/0868-3166/27/2/9615

TEMPERATURE DEPENDENCE OF ELASTIC AND ULTRASONIC PROPERTIES OF SODIUM BOROHYDRIDE

DEVRAJ SINGH[1], GIRIDHAR MISHRA[1,†], RAJKUMAR[2] AND RAJA RAM YADAV[3,4]

[1]*Department of Applied Physics, Amity School of Engineering and Technology, Bijwasan, New Delhi-110061, India*

[2]*Department of Physics, Gurgaon Institute of Technology and Management, Gurgaon-122413, India*

[3]*Department of Physics,University of Allahabad, Allahabad-211002, India*

[4]*Veer Bahadur Singh Purvanchal University, Jaunpur-222003, India*

[†]*E-mail:* giridharmishra@rediffmail.com

Received 10 April 2017
Accepted for publication 17 July 2017
Published 31 July 2017

Abstract. *We present the temperature dependent elastic and ultrasonic properties of sodium borohydride. The second and third order elastic constants of $NaBH_4$ have been computed in the temperature range 0-300K using Coulomb and Born-Mayer potentials. The sodium borohydride crystallizes into NaCl-type structure. The computed values of second order elastic constants have been applied to evaluate the temperature dependent mechanical properties such as bulk modulus, shear modulus, tetragonal modulus, Poisson's ratio and Zener anisotropy factor and ultrasonic velocity to predict futuristic information about sodium borohydride. The fracture to toughness ratio (bulk modulus/shear modulus) in sodium borohydride varied from 1.91 to 1.62, which shows its behavioral change from ductile to brittle on increasing the temperature. Then, ultrasonic Grüneisen parameters have been computed with the use of elastic constants in the temperature regime 100-300K. The obtained results have been discussed in correlation with available experimental and theoretical results.*

Keywords: sodium borohydride, elastic constants, mechanical properties, ultrasonic properties.

Classification numbers: 43.35.+d; 62.80.+f; 62.20.dq.

I. INTRODUCTION

The elastic and ultrasonic properties of solid materials have great interest for materials scientists and engineers since a long time. The elastic constants are key parameters to recognize

numerous physical properties of solids such as elasticity, mechanical stability, stiffness of materials, and the nature of forces operating within the solids. The temperature dependent study of the elastic constants is essential to envisage and know the material properties, such as its strength and mechanical stability [1]. Ultrasonic velocity is another key parameter in ultrasonic characterization of the materials and can provide information about the crystallographic texture. The ultrasonic velocity is directly related to the elastic constants and density of that particular material [2]. The mechanical properties play important role for providing future performance of the materials [3]. Ultrasonic Grüneisen parameters play a significant role in the study of thermo-elastic properties of materials [4].

Sodium borohydride ($NaBH_4$) is an important mild reducing agent. It has attracted many researchers in the area of reduction of functional groups to make advanced materials. One motive for the inconsistency between experimental and theoretical values of second order elastic constants is the obscurity in accounting for the anharmonicity and disorder in MBH_4 (M=Li, Na, K, Rb, Cs) [5]. The discrepancy between inelastic neutron scattering (INS) and Raman studies on the energy barrier for reorientation (librations) motion to anharmonicity have been ascribed by Hagemann *et al.* [6]. Filinchuk *et al.* [7] investigated crystal structure of $NaBH_4$ from synchrotron powder diffraction data in high pressure regime. Xiao-Ding *et al.* [8] presented higher order elastic constants computation of $NaBH_4$ based on ab-initio calculations and pointed out NaCl-type crystal structure of $NaBH_4$. A comprehensive study of structure, phase stability, optical and electronic properties of $NaBH_4$ have been presented by Ghellab *et al.* [9]. Bae *et al.* [10] studied effect of $NaBH_4$ on properties of nanoscale zero-valent iron and its catalytic activity for reduction of p-nitro phenol. Renaudin *et al.* [11] carried structural and spectroscopic investigations on the alkali borohydrides MBH_4. Vajeeston *et al.* [12] presented structural stability of alkali boron tetra hydrides MBH_4 from first principle calculation. Orimo *et al.* [13] studied synthesis, structural properties and future prospects of $NaBH_4$. Istek and Gonteki [14] studied utilization of $NaBH_4$ in Kraft pulping process. Kumar and Cornelinus [15] explored structural transition in $NaBH_4$ under pressure. Kim *et al.* [16] scrutinized pressure-induced structural transition in $NaBH_4$ through density functional theory computation with X-rays and neutron diffraction experiment.

However, the elastic, mechanical and ultrasonic studies have not been well interpreted for $NaBH_4$. This motivates us to study second and third order elastic constants, mechanical properties and ultrasonic properties of $NaBH_4$ in the temperature range 0-300K.

II. THEORY

II.1. Theory for the second- and third- order elastic constants

The theoretical formulation for the evaluation of second- and third- order elastic constants (SOECs and TOECs) was given by Brugger [17] first and then, successively developed by Ghate [18] and Mori and Hiki [19]. The SOECs and TOECs at particular temperature are obtained by adding the vibrational contribution to the static elastic constants as follows:

$$C_{IJ}(T) = C^0_{IJ} + C^{vib}_{IJ} \text{ and } C_{IJK}(T) = C^0_{IJK} + C^{vib}_{IJK} \tag{1}$$

where superscript 0 denotes static elastic constant at 0K and superscript *vib* denotes vibrational part of elastic constant at required temperature. The detailed expressions for SOECs and TOECs

for static and vibrational parts as in Eq. (1) are given below:

$$\left.\begin{aligned} C_{11}^{0} &= \tfrac{3}{2}\tfrac{e^2}{r_0^4}S_5^{(2)} + \tfrac{1}{br_0}\left(\tfrac{1}{r_0}+\tfrac{1}{b}\right)\varphi(r_0) + \tfrac{2}{br_0}\left(\tfrac{\sqrt{2}}{2r_0}+\tfrac{1}{b}\right)\varphi(\sqrt{2}r_0) \\ C_{12}^{0} &= C_{44}^{0} = \tfrac{3}{2}\tfrac{e^2}{r_0^4}S_5^{(1,1)} + \tfrac{1}{br_0}\left(\tfrac{\sqrt{2}}{2r_0}+\tfrac{1}{b}\right)\varphi(\sqrt{2}r_0) \end{aligned}\right\} \tag{2}$$

$$\left.\begin{aligned} C_{111}^{0} &= -\tfrac{15}{2}\tfrac{e^2}{r_0^4}S_7^{(3)} - \tfrac{1}{b}\left(\tfrac{3}{r_0^2}+\tfrac{3}{br_0}+\tfrac{1}{b^2}\right)\varphi(r_0) - \tfrac{1}{2b}\left(\tfrac{3\sqrt{2}}{r_0^2}+\tfrac{6}{br_0}+\tfrac{2\sqrt{2}}{b^2}\right)\varphi(\sqrt{2}r_0) \\ C_{112}^{0} &= C_{166}^{0} = -\tfrac{15}{2}\tfrac{e^2}{r_0^4}S_7^{(2,1)} - \tfrac{1}{4b}\left(\tfrac{3\sqrt{2}}{r_0^2}+\tfrac{6}{br_0}+\tfrac{2\sqrt{2}}{b^2}\right)\varphi(\sqrt{2}r_0) \\ C_{123}^{0} &= C_{144}^{0} = C_{456}^{0} = -\tfrac{15}{2}\tfrac{e^2}{r_0^4}S_7^{(1,1,1)} \end{aligned}\right\} \tag{3}$$

Here $\varphi(r_0)$ is the Born-Mayer inter-ionic potential model and given by

$$\phi(r_0) = A\exp\left(-\frac{r_0}{b}\right) \text{ and } \phi(\sqrt{2}r_0) = A\exp\left(-\frac{\sqrt{2}r_0}{b}\right) \tag{4}$$

where r_0 is the nearest-neighbor distance, b is hardness parameter and A is the strength parameter given by

$$A = -3b\frac{e^2}{r_0}S_3^{(1)}\frac{1}{6\exp(-\rho_0)+12\sqrt{2}\exp(-\sqrt{2}\rho_0)};\ \rho_0 = r_0/b \tag{5}$$

The vibrational contribution to the lattice is given by

$$\left.\begin{aligned} C_{11}^{vib.} &= f^{(1,1)}G_1^2 + f^{(2)}G_2 \\ C_{12}^{vib.} &= f^{(1,1)}G_1^2 + f^{(2)}G_{1,1} \\ C_{44}^{vib.} &= f^{(2)}G_{1,1} \end{aligned}\right\}$$

$$\left.\begin{aligned} C_{111}^{vib.} &= f^{(1,1,1)}G_1^3 + 3f^{(2,1)}G_1G_2 + f^{(2)}G_3 \\ C_{112}^{vib.} &= f^{(1,1,1)}G_1^3 + f^{(2,1)}G_1(2G_{1,1}+G_2) + f^{(3)}G_{2,1} \\ C_{123}^{vib.} &= f^{(1,1,1)}G_1^3 + 3f^{(2,1)}G_1G_{1,1} + f^{(3)}G_{1,1,1} \\ C_{144}^{vib.} &= f^{(2,1)}G_1G_{1,1} + f^{(3)}G_{1,1,1} \\ C_{166}^{vib.} &= f^{(2,1)}G_1G_{1,1} + f^{(3)}G_{2,1} \\ C_{456}^{vib.} &= f^{(2)}G_{1,1,1} \end{aligned}\right\} \tag{6}$$

where $f^{(n)}$ and G_n are given as:

$$f^{(2)} = f^{(3)} = \frac{h\omega_0}{8r_0^3}\coth x;$$

$$f^{(1,1)} = f^{(2,1)} = \frac{h\omega_0}{96r_0^3}\left(\frac{h\omega_0}{2kT\sinh^2 x}+\coth x\right)$$

$$f^{(1,1,1)} = \frac{h\omega_0}{384r_0^3}\left(\frac{(h\omega_0)^2\coth x}{6(kT)^2\sinh^2 x}+\frac{h\omega_0}{2kT\sinh^2 x}+\coth x\right)$$

$$
\begin{aligned}
G_1 =& 2\left\{\left(2+2\rho_0-\rho_0^2\right)\varphi(r_0)+2\left(\sqrt{2}+2\rho_0-2\rho_0^2\right)\varphi(\sqrt{2}r_0)\right\}H\\
G_2 =& 2\left\{\left(-6-6\rho_0-\rho_0^2+\rho_0^3\right)\varphi(r_0)+(-3\sqrt{2}-6\rho_0-\sqrt{2}\rho_0^2+2\rho_0^3)\varphi(\sqrt{2}r_0)\right\}H\\
G_3 =& 2\Big[\left(30+30\rho_0+9\rho_0^2-\rho_0^3-\rho_0^4\right)\varphi(r_0)\\
&+\left\{(15/2)\sqrt{2}+15\rho_0+(9/2)\sqrt{2}\rho_0^2-\rho_0^3-\sqrt{2}\rho_0^4)\right\}\varphi(\sqrt{2}r_0)\Big]H\\
G_{1,1} =& \left\{\left(-3\sqrt{2}-6\rho_0-\sqrt{2}\rho_0^2+2\rho_0^3\right)\varphi(\sqrt{2}r_0)\right\}H\\
G_{2,1} =& \left\{\left(\frac{15}{2}\sqrt{2}+15\rho_0+(9/2)\sqrt{2}\rho_0^2-\rho_0^3-\sqrt{2}\rho_0^4\right)\varphi(\sqrt{2}r_0)\right\}H,\\
G_{1,1,1} =& 0
\end{aligned}
$$

Here,

$$
\begin{aligned}
x =& h\omega_0/2kT,\\
\omega_0^2 =& \left(\frac{1}{M_+}+\frac{1}{M_-}\right)\left(\frac{1}{Hbr_0}\right),\\
H =& \left\{(\rho_0-2)\varphi(r_0)+2(\rho_0-\sqrt{2})\varphi(\sqrt{2}r_0)\right\}^{-1},
\end{aligned}
$$

k is the Boltzmann's constant, h is the Planck's constant and values of lattice sums are:

$$
\begin{aligned}
&S_3^{(1)}=-0.58252; \quad S_5^{(2)}=-1.04622; \quad S_5^{(1,1)}=0.23185\\
&S_7^{(3)}=-1.36852; \quad S_7^{(2,1)}=0.16115; \quad S_7^{(1,1,1)}=-0.09045
\end{aligned}
$$

II.2. Mechanical properties

The achieved results of elastic constants have been applied to compute the mechanical constants [20] like bulk modulus (B), shear modulus (G), tetragonal modulus (C_S), Poisson's ratio (σ) and Zener anisotropic ratio (A) using following formulae:

$$
\begin{aligned}
&B=\tfrac{C_{11}+2C_{12}}{3}; \quad G_V=\tfrac{C_{11}-C_{12}+3C_{44}}{5}; \quad G_R=\tfrac{5[(C_{11}-C_{12})C_{44}]}{4C_{44}+3(C_{11}-C_{12})}; \quad G=\tfrac{G_V+G_R}{2};\\
&C_S=\tfrac{C_{11}-C_{12}}{2}; \quad \sigma=\tfrac{3B-2G}{6B+2G}; \qquad\qquad A=\tfrac{2C_{44}}{C_{11}-C_{12}}
\end{aligned}
\tag{7}
$$

II.3. Ultrasonic velocities

When sound wave propagates through a solid medium, there are three modes of propagation one longitudinal acoustical and two transverse acoustical. Hence, there exist three types of velocities as one longitudinal (V_L) and two shear (V_{S1} and V_{S2}) that depend on the direction of propagation of wave [21]. The expressions for direction dependent ultrasonic velocities in cubic crystals are as follows:

Along $\langle 100\rangle$ crystallographic direction;

$$
V_L=\sqrt{\frac{C_{11}}{d}}; \quad V_{S1}=V_{S2}=\sqrt{\frac{C_{44}}{d}} \tag{8}
$$

Along $\langle 110 \rangle$ crystallographic direction;

$$V_L = \sqrt{\frac{C_{11}+C_{12}+2C_{44}}{2d}}; \quad V_{S1} = \sqrt{\frac{C_{44}}{d}}; \quad V_{S2} = \sqrt{\frac{C_{11}-C_{12}}{d}} \tag{9}$$

Along $\langle 111 \rangle$ crystallographic direction;

$$V_L = \sqrt{\frac{C_{11}+2C_{12}+4C_{44}}{3d}}; \quad V_{S1} = V_{S2} = \sqrt{\frac{C_{11}-C_{12}+C_{44}}{3d}} \tag{10}$$

The ultrasonic velocities can be computed using calculated values of second order elastic constants. The Debye average velocity (V_D) is useful for knowledge of thermal relaxation mechanisms of the materials. The following expressions have been used for evaluation of Debye average velocity [21].

$$\begin{aligned} V_D &= \left[\frac{1}{3}\left\{\frac{1}{V_L^3}+\frac{2}{V_{S1}^3}\right\}\right]^{-1/3} \text{; along } \langle 100 \rangle \text{ and } \langle 111 \rangle \text{ direction} \\ &= \left[\frac{1}{3}\left\{\frac{1}{V_L^3}+\frac{1}{V_{S1}^3}+\frac{1}{V_{S2}^3}\right\}\right]^{-1/3} \text{; along } \langle 110 \rangle \text{ direction} \end{aligned} \tag{11}$$

II.4. Ultrasonic Grüneisen parameters

A number of anharmonic properties of solids are frequently expressed in terms of ultrasonic Grüneisen parameters (UGPs) [4], which are expressed in quasi-harmonic approximation, as diverse weighted averages of Grüneisen tensor of first order $\gamma_{\alpha\beta}^{j} = \left(-\omega_i^{-1}\partial\omega_i(q)\right)/\partial\eta_{\alpha\beta}$. For example, the thermal expansivity is relative to the specific heat weighted $\langle \gamma_{\alpha\beta} \rangle = \sum_{q,i} C_{q,i}\gamma_{\alpha\beta}^{j} / \sum_{q,i} C_{q,i}$, which is the thermal Grüneisen parameter. The shear ultrasonic attenuation's Grüneisen parameter can be suitably expressed by the thermal conductivity weighted average of the product $\gamma_{\alpha\beta}^{j}\gamma_{\gamma\delta}^{j}$. Brugger [22] derived expressions for the components of Grüneisen tensor in terms of SOECs and TOECs of an anisotropic continuum. The UGPs have different modes of propagation along $\langle 100 \rangle$, $\langle 110 \rangle$ and $\langle 111 \rangle$ direction for getting average values of these. Expression [23] for computing UGPs are given in Appendices I-VII.

III. RESULTS AND DISCUSSION

Taking nearest neighbor distance (r_0 = 3.07 Å) [8] and hardness parameter ($b = 0.305$ Å) [24], the SOECs and TOECs have been computed using Eqs. (1)- (6) and are presented in Table 1. We compared our results for SOECs with experimental results of Nakamori and Orimo [25] and theoretical results of Xiao-Ding *et al.* [8]. It is depicted from Table 1 that our results are in good agreement with both above mentioned results. Table 1 depicts that the values of C_{11}, C_{44}, C_{111}, C_{166} and C_{144} increase 11.7%, 1.66%, 4.28%, 1.64% and 2.63% respectively and the values of C_{12}, C_{112} and C_{123} decrease 11.5%, 8.97% and 35.9% respectively from temperatures 0K to 300K. The value of C_{456} remains constant. The increase or decrease in elastic constants is due to increase or decrease in atomic interaction with temperature. If interatomic distance increase or decrease with temperature, then interaction potential decreases or increases, a result that causes, the decrease or increase in elastic constants. This type of nature of SOECs and TOECs is very similar to other

NaCl-type materials like thulium monochalcogenides [26], europium monochalcogenides [27] and neptunium monopnictides [28].

Table 1. Temperature dependent SOECs and TOECs of $NaBH_4$ [GPa].

Temp.(K)	C_{11}	C_{12}	C_{44}	C_{111}	C_{112}	C_{123}	C_{144}	C_{166}	C_{456}
0	25.29	11.39	11.39	-385.2	-46.70	17.87	17.87	-46.70	17.87
100	26.98	10.96	11.47	-395.5	-45.32	15.73	18.03	-47.10	17.87
200	27.77	10.52	11.52	-397.9	-43.94	13.58	18.18	-47.26	17.87
300	28.73	10.08	11.58	-401.7	-42.51	11.44	18.34	-47.47	17.87
300[8]	30.61	13.73	14.94	-351.1	-52.80	47.37	23.81	-66.86	13.75
300[25]	26.5	9.50	9.40						

It is proposed that the Cauchy relation [28] for SOECs and TOECs at 0K are:

$$C_{12}^0 = C_{44}^0 ; C_{112}^0 = C_{166}^0 ; C_{123}^0 = C_{456}^0 = C_{144}^0 \tag{12}$$

The Cauchy relations hold good at 0K and deviate as we go for high temperatures as seen in Table 1. This shows that the forces become more ionic with the rise of temperature.

The obtained results of SOECs and TOECs are applied to compute the bulk modulus (B), shear modulus (G), tetragonal moduli (C_S), Poisson's ratio (σ), Zener anisotropy factor (A) and ratio B/G using Eq. (7). These values are listed in Table 2 in the temperature range 0K to 300K.

Table 2. Temperature dependent B, G, Cs, σ, A and B/G of $NaBH_4$.

Temp. (K)	B (GPa)	G (GPa)	Cs (GPa)	σ	A	B/G
0	18.0	9.3	7.0	0.93	2.00	1.91
100	16.3	9.2	8.0	0.87	1.43	1.78
200	16.3	9.6	8.6	0.82	1.34	1.70
300	16.3	10.1	9.3	0.78	1.24	1.62

The Born stability criterion is also satisfied by $NaBH_4$ i.e., $B_T = (C_{11}+2C_{12})/3 > 0$, $C_{44}\rangle$ 0, $C_S = (C_{11} - C_{12})/2 > 0$, so we can say that these materials are stable. The Poisson ratio (σ) provides the information regarding the characteristics of the bonding force against other elastic constants. For central forces, the Poisson ratio limit is given by $0.25 < \sigma < 0.5$. In the present case the values do not fall in this range, which reveals the inter-atomic forces as non-central [29]. According to Pugh [30] for

$$\frac{B}{G} > 1.75 \text{ (material is ductile) and } \frac{B}{G} < 1.75 \text{ (brittle).}$$

In our case for the material $NaBH_4$, the calculated values of B/G show that the ductile nature at 0K and 100K and this ratio confirms the brittle nature at temperatures 200K and 300K. Hence brittle behavior of material increases with temperature.

The ultrasonic velocities (V_L and V_S) can be obtained using SOECs and density of the materials for longitudinal and shear modes of propagation using Eqs. (8)- (10); the Debye average velocity (V_D) in turn is evaluated using related to longitudinal and shear wave velocities using Eq. (11). The computed values of V_L, V_S and V_D are presented in Table 3.

Table 3. Temperature and orientation dependent V_L, V_S and V_D (km/s) of $NaBH_4$.

Direction	Temp. [K]	V_L	V_{S1}	V_{S2}	V_D
$\langle 100 \rangle$	100	4.89	3.19	3.19	3.97
	200	4.96	3.19	3.19	3.99
	300	5.04	3.20	3.20	4.02
$\langle 110 \rangle$	100	5.19	3.19	3.77	3.38
	200	5.21	3.19	3.91	3.80
	300	5.24	3.20	4.02	3.86
$\langle 111 \rangle$	100	5.29	2.85	2.85	3.75
	200	5.29	2.91	2.91	3.82
	300	5.30	2.99	2.99	3.89

It is obvious from Table 3 that V_L, V_S and V_D increase with temperature. The direction dependent Debye average velocities for different temperatures are also visualized in Fig. 1.

From Fig. 1, it is found that the Debye average velocity is maximum along $\langle 100 \rangle$ direction and minimum along $\langle 110 \rangle$ direction at temperatures 100K, 200K and 300K. So $\langle 100 \rangle$ direction will be most appropriate for wave propagation for the chosen material $NaBH_4$. The Debye average velocity increases with the increase of temperature. This type of behavior of wave velocity for the chosen material is similar to other NaCl-type materials [31, 32].

The ultrasonic Grüneisen parameter (UGP) contributes significantly in the case of thermoelastic properties of the materials. UGP is applied to discuss different materials properties such as thermal expansion, temperature variation of elastic constants, thermal conductivity and ultrasonic attenuation. The temperature dependent ultrasonic Grüneisen parameters, which are obtained by SOECs and TOECs are presented in Table 4 for three directions $\langle 100 \rangle$, $\langle 110 \rangle$ and $\langle 111 \rangle$ at temperatures 100K, 200K and 300K using the formulae given in Appendices I-VII.

In Table 4, the notations are: the temperature dependent average UGPs $\langle \gamma_i^j \rangle_l$ for longitudinal wave, average square UGPs $\langle (\gamma_i^j)^2 \rangle_l$ for longitudinal wave, average square UGPs $\langle (\gamma_i^j)^2 \rangle_{s1}$ and $\langle (\gamma_i^j)^2 \rangle_{s2}$ for shear wave along $\langle 100 \rangle$, $\langle 110 \rangle$ and $\langle 111 \rangle$ directions, here shear wave along $\langle 100 \rangle$ is polarized along $\langle 100 \rangle$, shear wave along $\langle 110 \rangle$ is polarized along $\langle 001 \rangle$ and $\langle 1\bar{1}0 \rangle$ directions and shear wave along $\langle 111 \rangle$ direction is polarized along $\langle \bar{1}10 \rangle$ direction. The values of average UGPs is

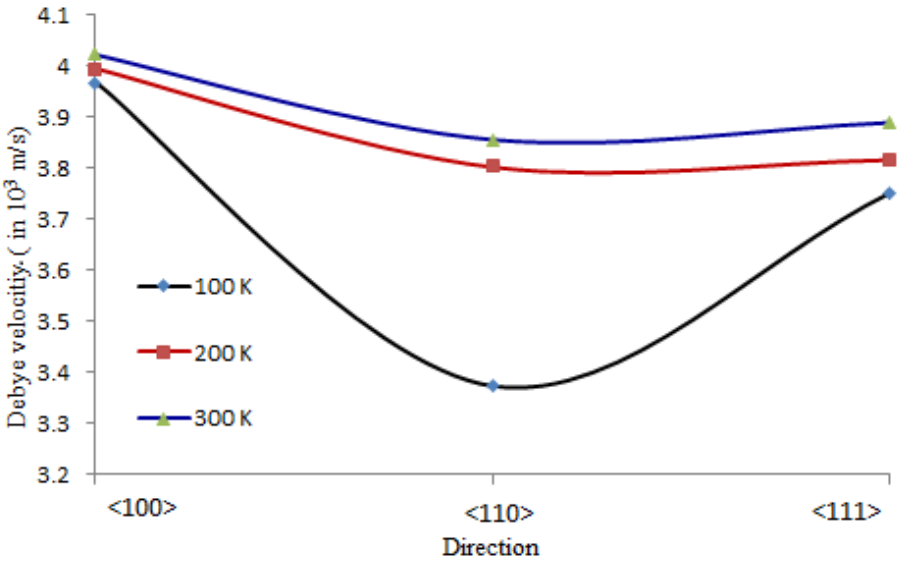

Fig. 1. Temperature and orientation dependent Debye velocity (km/s) of $NaBH_4$.

Table 4. Temperature and orientation dependent ultrasonic Grüneisen parameters of $NaBH_4$.

Direction	Temp. (K)	$\langle\gamma_i^j\rangle_l$	$\langle(\gamma_i^j)^2\rangle_l$	$\langle(\gamma_i^j)^2\rangle_{s1}$	$\langle(\gamma_i^j)^2\rangle_{s2}$
$\langle 100\rangle$	100	0.47	1.66	0.13	0.13
	200	0.45	1.54	0.12	0.12
	300	0.42	1.42	0.12	0.12
$\langle 110\rangle$	100	-0.79	2.26	0.15	2.52
	200	-0.75	2.05	0.14	2.40
	300	-0.71	1.86	0.14	2.27
$\langle 111\rangle$	100	-0.68	2.14	1.73	1.73
	200	-0.64	1.91	1.65	1.65
	300	-0.60	1.71	1.57	1.57

largest along $\langle 100\rangle$ direction at temperature 100K and lowest along $\langle 110\rangle$ direction at temperature 100K, while the average squared UGPs is largest along $\langle 111\rangle$ direction at temperature 100K for longitudinal wave and lowest along $\langle 100\rangle$ direction at temperature 300K for shear wave polarized along $\langle 100\rangle$ direction. The values of ultrasonic Grüneisen parameters decrease with increase of temperature. The nature of Grüneisen parameters seems to be same as the ones in previously studied NaCl-type berkelium monopnictides [21].

IV. CONCLUSIONS

Above discussion provides following information about sodium borohydride:

- The Coulomb and Born-Mayer potentials have been successfully applied for $NaBH_4$.
- Born criterion of stability has been satisfied by $NaBH_4$.
- The deviation of Cauchy's relation is found at higher temperatures.
- The value of Poisson's ratio does not fall in the regime of central force. So acting forces on $NaBH_4$ are non-central.
- Brittle nature of $NaBH_4$ increases with increase in temperature.
- The longitudinal and shear wave velocities increase with increase in temperature.
- The Debye average velocity is maximum along $\langle 100 \rangle$ direction, which shows most suitability along this direction.
- The decrement of values in Grüneisen parameters with temperature shows that $NaBH_4$ will perform better at low temperature.

Thus, our theoretical approach to compute higher order elastic constants, mechanical properties, ultrasonic velocities and ultrasonic Grüneisen parameters is justified. The obtained results of the present study can be used for further study of $NaBH_4$ to make it for futuristic applications.

ACKNOWLEDGEMENTS

Two of us (DS and GM) wish to express sincere thanks to Dr. Ashok K. Chauhan, Founder President; Prof. D.K. Bandyopadhyay, Chairman and Prof. Rekha Agarwal, Director, ASET, Bijwasan, New Delhi for their continuous encouragement and providing necessary facilities to complete this work. Authors are also grateful to Mr. Shobhit for reading the manuscript.

REFERENCES

[1] A. Amudhavalli, M. Manikandan, A. JemmyCinthia, R. Rajeswarapalanichamy and K. Iyakutti, *Z. Naturforsch. A* **72** (2017) 321.
[2] D. Singh, P. K. Yadawa and S. K. Sahu, *Cryogenics* **50** (2010) 476.
[3] V. Bhalla, D. Singh and S. K. Jain, *Int. J. Comput. Mat. Sc. Eng.* **5** (2016) 1650012.
[4] S. Kaushik, D. Singh and G. Mishra, *Asian J. Chem.* **24** (2012) 5655.
[5] D. Chernyshov, A. Bosak, V. Dmitriev, Y. Filinchuk and H. Hagemann, *Phys. Rev.B* **78** (2008) 172104.
[6] H. Hagemann, S. Gomes, G. Renaudin and K. Yvon, *J. Alloys Compd.* **363** (2004) 126.
[7] Y. Filinchuk, D. Chernyshov and V. Dmitriev, *Z. Kristallogr.* **223** (2008) 649.
[8] Z.Xiao Dong, J. Z. Yi, Z. Bo, H. Z. Feng and H. Y. Qing, *Chin. Phys. Lett*. **28** (2011) 076201.
[9] T. Ghellab, Z. Charifi, H. Baaziz, S. Uğur, G. Uğur and F. Soyalp, *Phys. Scr.* **91** (2016) 045804.
[10] S. Bae, S. Gim, H. Kim and K. Hanna, *Appl. Catal. B: Environm.* **182**(2016) 541.
[11] G. Renaudin, S. Gomes, H. Hagemann, L. Keller and K. Yvon, *J Alloys Compd.* **375** (2004) 98.
[12] P. Vajeeston, P. Ravindran, A. Kjekshus and H. Fjellvåg, *J Alloys Compd.* **387**(2005) 97.
[13] S. Orimo, Y. Nakamori, J. R. Eliseo, A. Zuttel and C. M. Jensen, *Chem. Rev.* **107** (2007) 4111.
[14] A. Istek and E. Gonteki, *J. Environm. Bio.* **7** (2009) 951.
[15] R. S. Kumar and A. L. Cornelinus, *Appl. Phys. Lett.* **87** (2005) 261916.
[16] E. Kim, R. Kumar, P. F. Weck, A. L. Cornelius, M. Nicol, S. C. Vogel, J. Zhang, M. Hartl, A. C. Stowe,L. Daemen and Y. Zhao, *J. Phys. Chem. Lett. B* **111** (2007) 13873.
[17] K. Brugger, *Phys. Rev.* **133** (1964) A1611.
[18] P. B. Ghate, *Phys. Rev*. **139** (1965) A1666
[19] S. Mori, Y. Hiki, *J. Phys. Soc. Jpn.* **45** (1975) 1449.

[20] V. Bhalla, R. Kumar, C. Tripathy and D. Singh, *Int. J. Mod. Phys. B* **27** (2013) 1350116.
[21] D. Singh, S. Kaushik, S. Tripathi, V. Bhalla and A. K. Gupta, *Arab. J. Sci. Eng.* **39** (2014) 485.
[22] K. Brugger, *Phys. Rev.* **137**(1965) 1826.
[23] W. P. Mason, *Physical Acoustics*, vol. IIIB, Academic Press, New York, 1965.
[24] M. P. Tosi, *Solid State Physics,*vol. 12, Academic Press, New York,1965.
[25] Y. Nakamori and S. Orimo, *J. Alloy Compd*. **370**(2004) 271.
[26] D. Singh, D. K. Pandey and P. K. Yadawa, *Cent. Eur. J. Phys.* **7** (2009) 198.
[27] V. Bhalla, D. Singh, G. Mishra and M. Wan, *J. Pure Appl. Ultrason*. **38**(2016) 23.
[28] D. Singh, S. Kaushik, S. K. Pandey, G. Mishra and V. Bhalla, *VNU J. Sc.: Math. Phys.* **32**(2016) 43.
[29] J.P.Watt and L. Peselnick, *J.Appl. Phys.* **51** (1980) 1525.
[30] S.F.Pugh, *Philos.Mag.* **45** (1954) 823.
[31] V. Bhalla, D. Singh and S. K. Jain, *Int. J. Thermophys*. **37**(2016) 33.
[32] V. Bhalla, D. Singh, S. K. Jain and R. Kumar, *Pramana- J. Phys.* **86** (2016) 135.

Appendix I. Grüneisen numbers along $\langle 100 \rangle$ for longitudinal waves:

Type of wave	No. of Modes	Equations for $\langle \gamma_i^j \rangle$
Longitudinal	1	$-\frac{3C_{11}+C_{111}}{2C_{11}}$
Shear	2	$-\frac{C_{11}+C_{166}}{2C_{44}}$
Longitudinal	2	$-\frac{C_{11}+C_{112}}{2C_{11}}$
Shear	2	$-\frac{2C_{44}+C_{12}+C_{166}}{2C_{44}}$
Shear	2	$-\frac{C_{12}+C_{144}}{2C_{44}}$
Longitudinal	2	$-\frac{2C_{12}+C_{112}+2C_{144}+C_{123}}{2(C_{11}+C_{12}+2C_{44})}$
Shear	2	$-\frac{2C_{12}+C_{112}-C_{123}}{2(C_{11}-C_{12})}$
Shear	2	$-\frac{C_{12}+2C_{44}+C_{166}}{2C_{44}}$
Longitudinal	4	$-\frac{2(C_{11}+C_{12}+C_{44})+C_{111}/2+3C_{112}/2+2C_{166}}{2(C_{11}+C_{12}+2C_{44})}$
Shear	4	$-\frac{2C_{11}+(C_{111}-C_{112})/2}{2(C_{11}-C_{12})}$
Shear	4	$-\frac{C_{11}+C_{12}+C_{144}+C_{166}}{4C_{44}}$
Longitudinal	4	$-\frac{5C_{11}+10C_{12}+8C_{44}+C_{111}+6C_{112}+2C_{123}+4C_{144}+8C_{166}}{6(C_{11}+2C_{12}+4C_{44})}$
Shear	4	$-\frac{4C_{11}+5C_{12}+C_{44}+(C_{111}+3C_{112})/2+(C_{144}+5C_{166})/2-2C_{123}}{6(C_{11}-C_{12}+C_{44})}$
Shear	4	$-\frac{2C_{11}+C_{12}+C_{44}+(C_{111}-C_{112})/2+(C_{144}+C_{166})/2}{2(C_{11}-C_{12}+C_{44})}$

Appendix II. Grüneisen numbers along $\langle 100 \rangle$ direction for shear waves and polarized along $\langle 100 \rangle$ direction.

Type of wave	No. of Modes	Equations for $\langle \gamma_i^j \rangle$
Longitudinal	2	$\pm\frac{C_{11}+C_{12}+C_{44}+C_{166}}{2(C_{11}+C_{12}+2C_{44})}$
Shear	2	$\pm\frac{C_{44}+C_{456}}{2C_{44}}$
Shear	2	$\pm\frac{C_{12}-C_{11}+2C_{44}}{2(C_{11}-C_{12})}$
Longitudinal	4	$\pm\frac{2C_{11}+4C_{12}+14C_{44}+4C_{144}+8C_{166}+8C_{456}}{6(C_{11}+2C_{12}+4C_{44})}$
Shear	4	$\pm\frac{2C_{11}+2C_{12}+4C_{44}-(C_{144}+2C_{456})+C_{166}}{6(C_{11}-C_{12}+C_{44})}$
Shear	4	$\pm\frac{2C_{44}-C_{144}+C_{166}}{2(C_{11}-C_{12}+C_{44})}$

Appendix III. Grüneisen numbers along $\langle 110 \rangle$ for longitudinal waves.

Type of wave	No. of Modes	Equations for $\langle \gamma_i^j \rangle$
Longitudinal	2	$\frac{3C_{11}+C_{12}+C_{111}+C_{112}}{4C_{11}}$
Shear	1	$\frac{2C_{11}+2C_{112}}{4C_{11}}$
Longitudinal	2	$\frac{C_{11}+C_{12}+2C_{44}+2C_{166}}{4C_{44}}$
Shear	2	$\frac{2C_{12}+2C_{44}+C_{144}+C_{166}}{4C_{44}}$
Shear	2	$\frac{C_{11}+C_{12}+C_{144}+C_{166}}{2C_{44}}$
Longitudinal	4	$\frac{2C_{11}+4C_{12}+2C_{44}+(C_{111}+5C_{112})/2+2C_{144}+2C_{166}}{4(C_{11}+C_{12}+2C_{44})}$
Longitudinal	1	$\frac{5C_{11}+5C_{12}+7C_{44}+C_{111}+3C_{112}+8C_{166}}{4(C_{11}+C_{12}+2C_{44})}$
Longitudinal	1	$\frac{3C_{11}+3C_{12}-3C_{44}+C_{111}+3C_{112}}{4(C_{11}+C_{12}+2C_{44})}$
Shear	4	$\frac{2C_{11}+2C_{12}+(C_{111}+C_{112})/2-C_{123}}{4(C_{11}-C_{12})}$
Shear	1	$\frac{3C_{11}+C_{12}+2C_{44}+C_{111}-C_{112}}{4(C_{11}-C_{12})}$
Shear	1	$\frac{3C_{11}-C_{12}-2C_{44}+C_{111}-C_{112}}{4(C_{11}-C_{12})}$
shear	1	$\frac{3C_{11}+2C_{12}+2C_{44}+2C_{144}+2C_{166}+2C_{456}}{8C_{44}}$
Shear	1	$\frac{C_{11}+3C_{12}+4C_{44}+C_{144}+3C_{166}}{8C_{44}}$
Shear	1	$\frac{2C_{11}+2C_{12}-2C_{44}+2C_{144}+2C_{166}-2C_{456}}{8C_{44}}$
Shear	2	$\frac{6C_{11}+12C_{12}+15C_{44}+C_{111}+6C_{112}+2C_{123}+6C_{144}+12C_{166}+4C_{456}}{6(C_{11}+2C_{12}+4C_{44})}$
Shear	2	$\frac{4C_{11}+8C_{12}+C_{44}+C_{111}+6C_{112}+2C_{123}+2C_{144}+4C_{166}-4C_{456}}{6(C_{11}+2C_{12}+4C_{44})}$
Longitudinal	2	$\frac{9(C_{11}+C_{12}+C_{44})+C_{111}+3C_{112}-3C_{144}+9C_{166}-4C_{456}}{12(C_{11}-C_{12}+C_{44})}$
Longitudinal	2	$\frac{7C_{11}+11C_{12}-5C_{44}+C_{111}-C_{112}+C_{144}+C_{166}-4C_{123}}{12(C_{11}-C_{12}+C_{44})}$
Shear	2	$\frac{3(C_{11}+C_{12}+C_{44})+C_{111}-C_{112}+C_{144}+C_{166}-C_{456}}{4(C_{11}-C_{12}+C_{44})}$
Shear	2	$\frac{5C_{11}+C_{12}+C_{44}+C_{111}-C_{112}+C_{144}+C_{166}+C_{456}}{4(C_{11}-C_{12}+C_{44})}$

Appendix IV. Grüneisen numbers shear waves propagating along $\langle 110 \rangle$ direction and polarized along $\langle 001 \rangle$ direction.

Type of wave	No. of Modes	Equations for $\langle \gamma_i^j \rangle$
Longitudinal	4	$\pm\frac{C_{11}+C_{12}+4C_{44}+4C_{166}}{2\sqrt{2}(C_{11}+C_{12}+2C_{44})}$
Shear	4	$\pm\frac{C_{11}-C_{12}-2C_{44}}{2\sqrt{2}(C_{11}-C_{12})}$
Shear	4	$\pm\frac{C_{44}+C_{456}}{2\sqrt{2}C_{44}}$
Longitudinal	2	$\pm\frac{2C_{11}+4C_{12}+14C_{44}+4C_{144}+8C_{166}+8C_{456}}{3\sqrt{2}(C_{11}+2C_{12}+4C_{44})}$
Shear	2	$\pm\frac{2C_{11}-2C_{12}-4C_{44}+C_{144}-C_{166}+2C_{456})}{3\sqrt{2}(C_{11}-C_{12}+C_{44})}$
Shear	4	$\pm\frac{2C_{44}-C_{144}+C_{166}}{\sqrt{2}(C_{11}-C_{12}+C_{44})}$

Appendix V. Grüneisen numbers shear waves propagating along $\langle 110 \rangle$ direction and polarized along $\langle 1\bar{1}0 \rangle$ direction.

Type of wave	No. of Modes	Equations for $\langle \gamma_i^j \rangle$
Longitudinal	2	$\pm\frac{3C_{11}-C_{12}+C_{111}-C_{112}}{2C_{11}}$
Shear	2	$\pm\frac{C_{11}-C_{12}-2C_{44}}{2C_{44}}$
Shear	2	$\pm\frac{2C_{44}-C_{144}+C_{456}}{2C_{44}}$
Shear	2	$\pm\frac{C_{11}-C_{12}-C_{144}+C_{166}}{2C_{44}}$
Longitudinal	4	$\pm\frac{2C_{11}+2C_{44}+(C_{111}+C_{112})/2-C_{123}-2C_{144}+2C_{166}}{2(C_{11}+C_{12}+2C_{44})}$
Shear	2	$\pm\frac{2C_{11}-2C_{12}+(C_{111}-3C_{112})/2+C_{123}}{2(C_{11}-C_{12})}$
Shear	4	$\pm\frac{C_{11}-C_{12}-4C_{44}+C_{144}-C_{166}}{4C_{44}}$

Appendix VI. Grüneisen numbers along $\langle 111 \rangle$ for longitudinal waves.

Type of wave	No. of Modes	Equations for $\langle \gamma_i^j \rangle$
Longitudinal	3	$\frac{3C_{11}+2C_{12}+C_{111}+2C_{112}}{6C_{11}}$
Shear	6	$\frac{C_{11}+2C_{12}+2C_{44}+2C_{166}+C_{144}}{6C_{44}}$
Longitudinal	3	$\frac{6C_{11}+8C_{12}+12C_{44}+C_{111}+4C_{112}+C_{123}+C_{144}+12C_{166}}{6(C_{11}+C_{12}+2C_{44})}$
Longitudinal	3	$\frac{2C_{11}+4C_{12}-4C_{44}+C_{111}+4C_{112}+C_{123}+2C_{144}-4C_{166}}{6(C_{11}+C_{12}+2C_{44})}$
Shear	3	$\frac{2C_{11}+4C_{12}+4C_{44}+C_{111}-C_{123}}{6(C_{11}-C_{12})}$
Shear	3	$\frac{6C_{11}-4C_{44}+C_{111}-C_{123}}{6(C_{11}-C_{12})}$
Shear	3	$\frac{C_{11}+2C_{12}+2C_{166}+C_{144}+2C_{456}}{6C_{44}}$
Shear	3	$\frac{C_{11}+2C_{12}+2C_{166}+C_{144}-2C_{456}}{6C_{44}}$
Longitudinal	1	$\frac{9C_{11}+18C_{12}+36C_{44}+C_{111}+4C_{112}+2C_{123}+12C_{144}+16C_{456}}{6(C_{11}+2C_{12}+4C_{44})}$
Longitudinal	3	$\frac{11C_{11}+22C_{12}-4C_{44}+3C_{111}+12C_{112}+6C_{123}+4C_{144}+8C_{166}-16C_{456}}{18(C_{11}+2C_{12}+4C_{44})}$
Shear	1	$\frac{3C_{11}+6C_{12}+12C_{44}+C_{111}-C_{123}-3C_{144}+6C_{166}-2C_{456}}{6(C_{11}-C_{12}+C_{44})}$
Shear	2	$\frac{13C_{11}+4C_{12}-8C_{44}+3C_{111}-3C_{123}+4C_{144}-2C_{166}-2C_{456}}{6(C_{11}-C_{12}+C_{44})}$
Shear	1	$\frac{25C_{11}+2C_{12}+4C_{44}+3C_{111}-3C_{123}-C_{144}-10C_{166}+10C_{456}}{18(C_{11}-C_{12}+C_{44})}$
Shear	1	$\frac{3C_{11}+6C_{12}+12C_{44}+C_{111}-C_{123}-3C_{144}+6C_{166}-2C_{456}}{6(C_{11}-C_{12}+C_{44})}$
Shear	2	$\frac{7C_{11}+2C_{12}+C_{111}-C_{123}-C_{144}+2C_{166}+2C_{456}}{6(C_{11}-2C_{12}+C_{44})}$
Shear	1	$\frac{3C_{11}+6C_{12}-4C_{44}+C_{111}-C_{123}+5C_{144}-2C_{166}-2C_{456}}{6(C_{11}-2C_{12}+C_{44})}$

Appendix VII. Grüneisen numbers shear waves propagating along $\langle 111 \rangle$ direction and polarized along $\langle \bar{1}10 \rangle$ direction.

Type of wave	No. of Modes	Equations for $\langle \gamma_i^j \rangle$
Longitudinal	2	$\pm\frac{3C_{11}-C_{12}+C_{111}-C_{112}}{\sqrt{6}C_{11}}$
Shear	2	$\pm\frac{C_{11}-C_{12}-2C_{44}}{\sqrt{6}C_{44}}$
Longitudinal	2	$\pm\frac{-5C_{11}-C_{12}-8C_{44}-C_{111}-8C_{166}-C_{112}+2C_{123}+4C_{144}}{2\sqrt{6}(C_{11}+C_{12}+2C_{44})}$
Shear	2	$\pm\frac{-3C_{11}+C_{12}-C_{111}-C_{112}+2C_{123}+4C_{144}}{2\sqrt{6}(C_{11}+C_{12}+2C_{44})}$
Shear	2	$\pm\frac{-C_{11}+3C_{12}-2C_{44}-C_{111}+3C_{112}-2C_{123}}{2\sqrt{6}(C_{11}-C_{12})}$
Shear	2	$\pm\frac{-5C_{11}+5C_{12}+2C_{44}-C_{111}+3C_{112}-2C_{123}}{2\sqrt{6}(C_{11}-C_{12})}$
Longitudinal	2	$\pm\frac{-C_{11}+C_{12}+3C_{44}-C_{144}+C_{166}-C_{456}}{2\sqrt{6}C_{44}}$
Shear	2	$\pm\frac{-C_{11}+C_{12}+5C_{44}-C_{144}+C_{166}-C_{456}}{2\sqrt{6}C_{44}}$
Shear	2	$\pm\frac{2C_{11}+4C_{12}+14C_{44}+4C_{144}+8C_{166}+8C_{456}}{3\sqrt{6}(C_{11}+2C_{12}+4C_{44})}$
Shear	2	$\pm\frac{-2C_{11}+2C_{12}+C_{44}-C_{144}-C_{166}-2C_{456}}{3\sqrt{6}(C_{11}-C_{12}+C_{44})}$
Shear	2	$\pm\frac{2C_{44}-C_{144}+C_{166}}{3\sqrt{6}(C_{11}-C_{12}+C_{44})}$
Longitudinal	2	$\pm\frac{C_{11}-C_{12}-C_{144}+C_{166}}{\sqrt{6}C_{44}}$
Longitudinal	2	$\pm\frac{2C_{44}-C_{144}+C_{166}}{\sqrt{6}C_{44}}$